Research Paper

# Tong Qiao Yizhi Granules Modulates the Synaptic Plasticity in Rats with Vascular Dementia by Activating MAPK/ERK/CREB Signalling Pathway

LAN CHEN, HUI TANG, LINGXUE WANG[1], SHUANGYANG LI[1], XUE BAI[1] AND HONGMEI TANG[1]*

Department of Neurology, [1]Department of Traditional Chinese Medicine, Traditional Chinese Medicine Affiliated Hospital of Southwest Medical University, Luzhou, Longmatan 646610, China

**Chen *et al.*: Role of Tong Qiao Yizhi Granules in Vascular Dementia Rats**

**Patients with vascular dementia are unable to live freely due to diminished cognitive function and daily life skills. It is vital to identify new medical therapies since, at the moment, anti-dementia medications only temporarily alleviate patients' clinical symptoms and have no impact on slowing the progression of the disease or enhancing the prognosis of the condition. In this work, a permanent bilateral common carotid artery blockage was used to create a rat model of vascular dementia. The rats that were effective at modeling were divided into four groups namely, model, high-dose Tong Qiao Yizhi granules group, medium-dose Tong Qiao Yizhi granules and memantine group. After 30 d of intragastric injection, the behavioral alterations in the rats in each group were noted. By using golgi staining, the density of dendritic spines was discovered. Further, hippocampus cornu ammonis 1 region's synapses' was examined using transmission electron microscopy. By using an immunofluorescence test, the glutamate receptor subunits expression levels in the hippocampus cornu ammonis 1 area were discovered. The expression of synaptic growth associated protein-43, synaptophysin and postsynaptic density protein 95; expression of important pathway components like mitogen activated protein kinase enzymes 1/2, phospho-mitogen activated protein kinase enzymes, extracellular signal-regulated protein kinases 1/2, phospho-extracellular signal-regulated protein kinase and cyclic adenosine monophosphate response element binding protein/phospho-cyclic adenosine monophosphate response element binding protein were all detected in the hippocampus through Western blotting. The findings demonstrated that Tong Qiao Yizhi granules might enhance cognitive function and synaptic ultrastructure in the hippocampus cornu ammonis 1 area among the vascular dementia rats, as well as greatly increase the density of dendritic spines. We deduced that Tong Qiao Yizi granules can significantly enhance the learning and memory capacity of vascular dementia rats based on the aforementioned findings. The process may involve activating cyclic adenosine monophosphate response element binding protein to increase synaptic plasticity and upregulate the phosphorylation levels of mitogen activated protein kinase enzymes 1/2 and extracellular signal-regulated protein kinases 1/2 and important components of the mitogen activated protein kinases/extracellular signal-regulated kinase signaling pathway, in order to improve the memory impairment in vascular dementia rats.**

**Key words: Vascular dementia, Xuanfu theory, Tong Qiao Yizhi granules, mitogen-activated protein kinase, synaptic plasticity**

Vascular Dementia (VaD) is a neurodegenerative cognitive dysfunction syndrome defined by the loss in cognitive function and the capacity to carry out activities of daily life. It is caused by the dysregulation of cerebral blood flow and neurovascular injury; effected people are unable to live on their own[1]. The pathogenic processes of VaD may be roughly categorized into two groups, neurological damage brought on by extended exposure to different risk factors and brain damage which is brought on by various forms of ischemic or hemorrhagic events[2]. Events like ischemia and bleeding cause inflammatory reactions, oxidative stress and the release of excitatory neurotransmitter toxicity, all of which wreak havoc on nerve and neuronal tissue and impair cognition[3,4]. Cerebral vasculature is threatened by underlying conditions including hypertension, hyperlipidemia and diabetes, which can cause long-term hypoxia and reduced blood flow in the brain, which can damage the brain tissue

***Address for correspondence**
E-mail: hm1207@163.com

and culminate in VaD[5,6]. Cholinesterase inhibitors, antioxidants and calcium channel blockers are now the major 1st line anti-dementia medications. However, these medications only temporarily relieve the clinical symptoms of patients and have no impact on the prognosis or the disease's progress. Due to its effectiveness, lack of negative side effects and the use of several therapeutic targets, traditional Chinese medicine has attracted a lot of interest lately. Based on the Xuanfu theory explained by Wang, it can be considered that the pathogenesis of VaD is caused by the blockage of the brain's Xuanfu and the loss of clear orifices and the therapy is to open the occlusion of the brain's Xuanfu and restore the divine mechanism. Tong Qiao Yizhi Granules (TQYZG) are generated by combining the best parts of the formula for wind, warm and tonic medicines. By observing the behavioral and hippocampal synaptic morphological changes in rats using a VaD model, as well as by detecting the expression of Growth Associated Protein-43 (GAP-43), Synaptophysin (Syn) and Postsynaptic Density-95 (PSD-95), we investigated the mechanism of action of TQYZG on learning memory related to synaptic plasticity in VaD.

## MATERIALS AND METHODS

### Experimental animals and conditions:

120 male Sprague-Dawley (SD) adult rats weighing around (250-300) g were purchased from the Experimental Animal Centre of Southwest Medical University (production licence number: SCXK (Chuan) 2018-17 and 065). 5 rats/cage were housed and the experiment was conducted at constant temperature of 25±2°, humidity of 50 %-55 %, light/dark cycle for 12 h in a controlled and quiet environment with free access to food and water.

### Experimental drugs:

**Chinese medicinal preparation:** TQYZG were composed of 3 g of Dilong extract, 0.5 g of leech, 3 g of *Ganoderma lucidum*, 2 g of *ginseng*, 3 g of *Acorus calamus*, 3 g of Chuanxiong (*Ligusticum striatum*), 12 g of *Pueraria lobata* and 20 g of *Astragalus membranaceus*. The aforementioned herbs were purchased from Southwest Medical University's Hospital of Traditional Chinese Medicine and the department's chief herbalist has verified their authenticity. *Acorus* and leech were soaked in 70 % ethanol for 1 w before the percolation technique was carried out to extract the volatile oil. Following extraction, all of the herbs were decocted for 3 times and the leftover material was filtered and concentrated; 2 g/ml concentrated solution was made and stored in a cold environment.

**Positive control drug:** 10 mg/tablet of Memantine (MEM) hydrochloride tablets were compounded in a 1 mg/ml solution for gavage which were obtained from the Denmark Ling North (Batch no: 814816).

### Experimental reagents:

Phospho (p)-Mitogen-activated Protein Kinase 1 and 2 (MEK1/2) antibody (CST, 86128, United States of America (USA)); MEK1/2 antibody (CST, #4694, USA); p-Extracellular Signal-Regulated Kinase 1/2 (ERK1/2) antibody (CST, #9101, USA); ERK1/2 antibody (CST, #4695, USA); p-Cyclic adenosine monophosphate Response Element Binding (CREB) antibody (CST, #9198, USA); CREB antibody (CST, #9197, USA); PSD-95 antibody (CST, #3450, USA); GAP-43 antibody (Abcam, 75810); Syn antibody (Abcam, 212184); Glutamate N-methyl-D-aspartate (GluN1) receptor antibody (109182) Abcam, Inc.; Glutamate ionotropic (GluA2) receptor antibody (Abcam, 174785); GluN2B antibody (MyBioSource, 802940); goat anti-mouse Immunoglobulin G (IgG) Heavy and Light (H&L) chains Horseradish Peroxidase (HRP) (Abcam, 205719); goat anti-rabbit IgG H&L (HRP) (Abcam, 205718) and Glyceraldehyde-3-Phosphate Dehydrogenase (GAPDH) (Beijing Bioss Healing Biological Technology Co., Ltd.).

### Experimental method:

**Animal model and groups:** Common carotid arteries on both sides of the body were permanently blocked to create the VaD rat model[7], while the common carotid arteries were bluntly dissected only for the control group. Morris Water Maze (MWM) row placement navigation experiment, was utilized as the evaluation criterion on the 30th d of postoperation[8] and was used to screen VaD rats by utilizing the mean value of evasion latency in the sham group as A and Escape Latency (EL) value in each model group as B.

Mean=(B-A)/A×100 %

20 VaD mice were randomly assigned into 5 groups, sham, model, high and medium dosage TQYZG and MEM groups. Following successful modeling, each group received the medication once daily for 30 d at dosage of 9.68 g/kg/d for the high dose group, 4.84 g/kg/d for the medium dose group and 1.04

mg/kg/d for the MEM group. Double-distilled water was gavaged to rats in the model and sham groups in equal amounts at a rate of 3 ml/d.

**MWM test for evaluation of behavioral changes:**

MWM test was used to assess the learning ability of the rats where learning memory had changed on the 2nd d following the conclusion of the gavage. It was ensured that the surroundings are calm, dark which maintained standard reference. Platform was placed in quadrant III to begin the experiment and enough black ink was added to the water beforehand to cover the platform. Experiment on positioning and navigation was carried out from quadrant I to IV where the rats were submerged, facing the wall's side. Each rat was allowed a maximum of 90 s to find the submerged platform; if the rat found the platform, it was allowed to remain there for at least 3 s. Escape Latency (EL), is the time the rat takes to find the platform which was recorded. If the rat did not find the platform within 90 s, EL was recorded as 120 s. EL was recorded for each rat received training for 5 d consecutively.

Spatial exploration experiment was conducted on 6th d. The hidden platform was removed and the rats were released into any area. The period of time the rats swam in the target area and the number of times they swam around the original set-up platform was recorded within 120 s, once/d for 2 d.

**Neuronal dendritic spine staining:**

This test was carried out to assess the neuronal morphology. Seahorse tissues were fixed in a mordant solution at room temperature (avoiding light and replacing it daily), blotted dry with filter paper after 5 d, replaced by silver plating using 1.5 % silver nitrate solution. Plating solution was replaced daily, wrapped in tin foil and dip-dyed continuously for 1 w, avoiding light until there was no red precipitation. After rapid dehydration, the tissue blocks were embedded with fire cotton glue, sliced by a shock sectioning machine with a thickness of 50 μm, soaked in 2 % aqueous potassium dichromate solution and rinsed for 10 min. The sections were rinsed under running water, pasted on slides coated with 1 % gelatin, dried and dehydrated using an alcohol gradient (80 %, 90 %, 95 %, 100 % I and 100 % II ethanol) for 5 min each, followed by xylene permeabilization for 10 min, neutral gum sealing and drying for microscopic examination. The number of dendritic spines per 10 μm was determined using Image J software by dividing the apical and basal secondary branches of the base-most neurons.

**Electron microscopic inspection:**

The fixed hippocampal tissues were trimmed out in sections of approximately 1 $mm^3$ in size, fixed in glutaraldehyde, 1 % osmium acid for 2 h, rinsed twice with Phosphate Buffered Saline (PBS) solution, dehydrated by ethanol gradient, epoxy resin embedded for baking, sectioned with a 200-mesh copper mesh carrier, double-stained with uranyl acetate-lead citrate and then observed the synaptic ultrastructure of the hippocampal Cornu Ammonis (CA) 1 region by transmission electron microscopy.

**Immunofluorescence:**

The whole-brain tissue was removed, washed and rinsed under running water for 1 h. It was fixed in paraformaldehyde for 24 h, then dehydrated in gradient ethanol (70 %, 80 % and 90 %) for 1 h each followed by 95 %, 100 % I and 100 % II for 1.5 h). The tissue was incubated in transparent xylene I and II for 10 min each and was finally embedded. The sections were successively sectioned, baked, dewaxed and rehydrated (xylene I and II dewaxed, each graded alcohol hydration), repaired with sodium citrate antigen, sealed with 5 % sheep serum at 37° for 30 min. Then the tissue was incubated with primary antibody overnight at 4° in a light-proof wet box followed by incubation with secondary antibody for 1 h. Subsequently, the tissue was stained with 4',6-Diamidino-2-Phenylindole (DAPI) for nucleation and was sealed with neutral gum. After blocking, the expression of the hippocampus CA1 protein in the nucleus or cytoplasm was seen under a 400X fluorescent microscope, photographed and was recorded. Using Internet Printing Protocol (IPP) software and the Mean Optical Density (MOD) of the positive cells was calculated.

**Western blotting:**

Seahorse tissues were removed from the refrigerator (maintained at 80°) and weighed; the tissues were placed in 1 ml homogenization tubes, cut with ophthalmic scissors. They were further homogenized by adding lysis solution (on ice) and were left undisturbed for 10 min. The tissues were centrifuged at 4° for 15 min at 12 000 rpm. The supernatant was aspirated, protein concentration was measured by Bicinchoninic Acid (BCA) and the amount of sample was determined by Sodium Dodecyl Sulphate-Polyacrylamide Gel Electrophoresis (SDS-PAGE) configuration. The membrane was transferred by using

5 % Bovine Serum Albumin (BSA) and was blocked for 1 h; primary antibody incubation (MEK1/2) was carried out. After determining the amount of protein to be sampled, SDS-PAGE gel configuration was carried out followed by electrophoresis and membrane transfer. 5 % of BSA was used to block the membrane for 1 h followed by primary antibody incubation (MEK1/2 and p-MEK1/2 1:1000; ERK1/2 and p-ERK1/2 (1:2000); CREB and p-CREB (1:1000), and GAP-43, Syn and PSD-95 (1:1000). The membrane was allowed to shake overnight for (16-24) h at 4° and the membrane was washed 3 times with 1×Tris-Buffered Saline 0.1 % Tween® (TBST) for 10 min each. Further, the membrane was incubated with secondary antibodies at room temperature for 2 h (1:8000) and was subjected to 3 washes with 1×TBST for 10 min each. Finally, image acquisition was carried out in Image Lab system after Enhanced Chemiluminescence (ECL) development and grey scale values were measured by Image Pro PLUS 6.0 software.

**Statistical analysis:**

The experimental data was measured and the values of the experimental data variables were expressed as the mean±Standard Deviation ($\bar{x}$±SD). One-Way Analysis of Variance (ANOVA) was used for the comparison between the groups. Least Significant Difference (LSD) test was used if the variance was equal and Dunnett's test was used if the variance was not equal; p=0.05 was considered to be the test level value. Statistical Package for Social Sciences (SPSS) version 22.0 and Graph Pad Prism version 8.0 were used for data statistics and graphing.

## RESULTS AND DISCUSSION

Behavioural effects of TQYZG on VaD model rats were evaluated. The results of positional navigation tests performed on various rat groups before and after surgery were presented (Table 1).

Prior to surgery, there was no statistically significant difference in the mean EL values between the groups (p>0.05). There was no statistically significant difference between the EL values before and after 30 d of surgery in the sham-operated group (p>0.05) while there were varying degrees of increase in the EL values of the rats in each administration group compared to the sham-operated group (p<0.05).

Learning ability and the ability to remember gavage among the rats in different groups was studied. EL period significantly decreased in the sham, model and MEM groups in the positioning navigation experiment, and the scores stabilized on 5th d. Compared with the sham group, EL of the model group was significantly longer (p<0.05) (Table 2). Similarly, compared with the model group, EL of MEM was significantly shorter (p<0.05). TQYZG high-dose group was found to have most significantly shortened EL (p<0.05) while the TQYZG medium-dose and the MEM groups were not statistically significantly different (p>0.05) (fig. 1).

Spatial exploration experiment results evaluated that the number of times the model group and each drug administration group crossed the original platform was reduced (p<0.05), compared with the sham group and the time spent moving to quadrant III was shortened to varying degrees (p<0.05). Similarly, compared with the model group, the number of times each drug group crossed the platform and the time spent swimming in quadrant III was increased (p<0.05). This increase was distinct in the TQYZG high-dose group (p<0.05), while there was no significant difference between the TQYZG medium-dose group and MEM group relative to each other (p>0.05) (Table 3).

Further, the impact of TQYZG on the CA1 region of the hippocampus' synaptic structure in VaD rats and the effect on dendritic spine density in rat neurons were assessed. The dendritic structure of the neurons in the CA1 area was intact and neuronal dendritic spine staining showed that the density of the dendritic spine was higher in the sham-operated group while it was significantly lower in the model group compared to the sham group (p<0.001). Dendritic spine density was higher in the TQTZG and MEM groups compared to the model group (4.84 g/kg/d and 9.68 g/kg/d, respectively) (p<0.001). Significant improvement was seen in TQYZG high-dose group (p<0.05), while TQYZG medium-dose and MEM group showed no statistically significant improvement (p>0.05), which depicts that there was no statistical comparison between TQYZG medium-dose and MEM groups (p>0.05) (fig. 2 and Table 4).

Synaptic ultrastructural changes in the CA1 region of the rat hippocampus were studied. The synaptic gap in the rat hippocampus' CA1 region in sham group was clear. Outline of the anterior and posterior synaptic membranes was intact, with more synaptic vesicles and regular synaptic surface. Anterior and posterior synaptic membranes were well anastomosed, with abundant synaptic vesicles and uniform size; mitochondrial structure was intact with dense myelin sheath wall.

**TABLE 1: COMPARISON OF EL IN EACH GROUP OF RATS BEFORE AND 30 D AFTER THE OPERATION (n=20, x̄±s)**

| Group | Pre-operative (s) | 30 d post-operative (s) | t | p |
|---|---|---|---|---|
| Sham | 77.21±2.75 | 73.86±7.78 | 1.814 | 0.078 |
| Model | 72.47±16.08$^{\#}$ | 94.69±7.83$^{*+}$ | - | - |
| TQYZG high-dose | 79.23±2.40$^{\#}$ | 101.03±10.03$^{*+}$ | - | - |
| TQYZG medium-dose | 80.32±2.92$^{\#}$ | 100.63±7.76$^{*+}$ | - | - |
| MEM | 76.11±15.26$^{\#}$ | 106.16±7.21$^{*+}$ | - | - |
| F | 1.815 | 5.478 | - | - |
| p | 0.132 | 0.001 | - | - |

Note: $^{\#}$p>0.05 and *p<0.05 compared to the sham group and $^{+}$p>0.05 compared to the model group

**TABLE 2: RESULTS OF THE POSITIONING NAVIGATION EXPERIMENT FOR EACH GROUP (n=20, x̄±s)**

| Group | 1st d | 2nd d | 3rd d | 4th d | 5th d |
|---|---|---|---|---|---|
| Sham | 79.61±1.65 | 60.34±6.13 | 40.96±22.64 | 25.74±9.08 | 23.71±6.18 |
| Model | 81.63±3.37 | 76.23±5.34 | 71.53±23.08 | 53.38±11.20 | 48.01±5.91$^{*\blacklozenge\square}$ |
| TQYZG high-dose | 80.08±2.87 | 71.14±7.50 | 50.16±8.67 | 40.45±4.71 | 29.40±8.13$^{*\#\blacklozenge\square}$ |
| TQYZG medium-dose | 80.76±5.36 | 70.93±8.51 | 65.82±12.35 | 50.76±8.37 | 40.32±8.10$^{*\#+}$ |
| MEM | 79.11±5.94 | 72.67±10.15 | 65.74±12.79 | 46.87±9.94 | 40.96±10.04$^{*\#+}$ |
| F | 1.131 | 11.84 | 11.354 | 30.456 | 31.094 |
| p | 0.347 | <0.01 | <0.01 | <0.01 | <0.01 |

Note: *p<0.05 *vs*. sham group, $^{\#}$p<0.05 *vs*. model group, $^{+}$p<0.05 *vs*.TQYZG high dose group, $^{\blacklozenge}$p<0.05 *vs*. TQYZG medium-dose group and $^{\square}$p<0.05 *vs*. MEM group

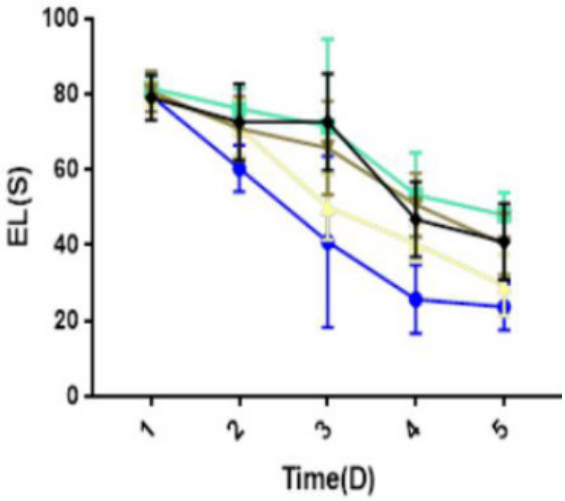


**Fig. 1: Results of positioning navigation experiment**

**TABLE 3: RESULTS OF THE SPATIAL EXPLORATION EXPERIMENT IN RATS (n=20, x̄±s)**

| Group | Number of platforms (times) | Target quadrant dwell time (s) |
|---|---|---|
| Sham | 34.70±3.45 | 60.30±6.61 |
| Model | 19.67±1.38$^{*+\blacklozenge\square}$ | 30.87±2.76$^{*+\blacklozenge\square}$ |
| TQYZG high-dose | 29.20±2.27$^{*\#\blacklozenge\square}$ | 50.87±5.47$^{*\#\blacklozenge\square}$ |
| TQYZG medium-dose | 25.20±1.75$^{*\#+}$ | 39.60±4.90$^{*\#+}$ |
| MEM | 24.45±2.08$^{*\#+}$ | 40.70±5.79$^{*\#+}$ |
| F | 119.909 | 92.597 |
| p | <0.01 | <0.01 |

Note: *p<0.05 *vs*. sham group, $^{\#}$p<0.05 *vs*. model group, $^{+}$p<0.05 *vs*.TQYZG high dose group, $^{\blacklozenge}$p<0.05 *vs*. TQYZG medium-dose group and $^{\square}$p<0.05 *vs*. MEM group

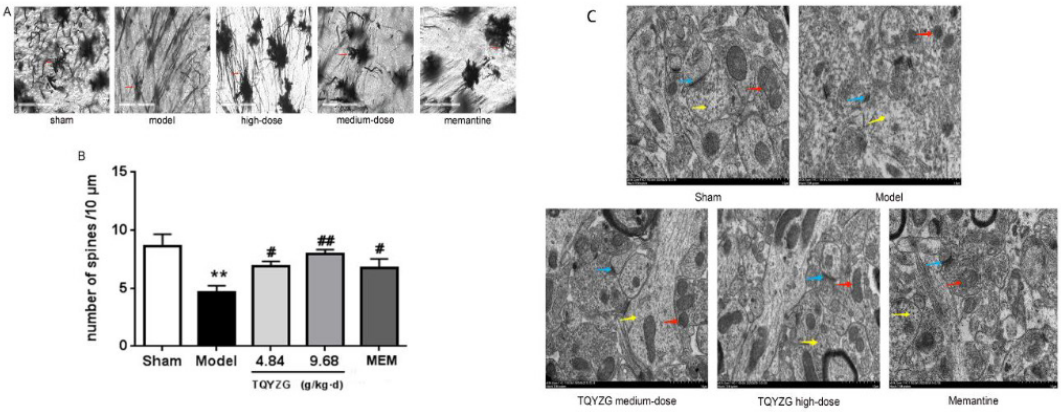


**Fig. 2: Results of neuronal dendritic spine staining, (A): CA1 region of the hippocampus, (B): Comparison of dendritic spine densities in various groups of rats and (C): Microscopic analysis of synaptic ultrastructure (8000X)**
**Note: ( ): Synaptic active zone; ( ): Mitochondria and ( ): Synapse**

**TABLE 4: COMPARISON OF DENDRITIC SPINE DENSITY IN THE CA1 REGION OF THE HIPPOCAMPUS OF RATS IN EACH GROUP (x̄±s)**

| Group | n | Density (μm) |
|---|---|---|
| Sham | 5 | 8.93±6.61 |
| Model | 5 | 4.67±0.53*+♦□ |
| TQYZG high-dose | 5 | 7.96±0.37*##♦□ |
| TQYZG medium-dose | 5 | 6.57±0.25*#+ |
| MEM | 5 | 6.41±0.25*#+ |
| F | - | 30.833 |
| p | - | <0.01 |

Note: *p<0.05 *vs*. sham group, #p<0.05 *vs*. model group, +p<0.05 *vs*.TQYZG high dose group, ♦p<0.05 *vs*. TQYZG medium-dose group and □p<0.05 *vs*. MEM group

Similarly, the synaptic gap was blurred with swollen pre- and post-synaptic membranes and cavitated in model group, making it difficult to distinguish the two. Synaptic vesicles were also reduced, with irregular and uniform morphology. The mitochondrial structure was shrunken and deformed while the myelin wall was thinner and looser and the length of the active zone was shorter.

TQYZG high-dose group had intact anterior and posterior synaptic membrane structure, clear synaptic gaps, more abundant synaptic vesicles with uniform morphology, increased active zone length, intact mitochondrial structure, increased number and thickened myelin sheath wall compared with the model group while TQYZG medium-dose group denoted incomplete anterior and posterior synaptic membrane structure, wider synaptic gap, shorter active zone with more intersynaptic vesicles, more regular and uniform morphology and more intact mitochondrial structural parts than the model group, but not as many as the high-dose group.

However, the anterior and posterior synaptic membrane structure was more complete in MEM group. The synaptic gap was slightly wider with shorter active zone. There were fewer intersynaptic synaptic vesicles with different and uneven morphology whose mitochondrial structure was irregular and intact. It was improved compared with the model group, but not as much as the medium-dose group (fig. 2C).

Effect of TQYZG on proteins in the synaptic membrane of VaD rats was explained using GluA2. In hippocampal tissues of rats, immunofluorescence showed that the expression of GluA2, GluN1 and GluN2B was significantly lower in the model group compared to the sham group (fig. 3). In contrast, the expression of GluA2, GluN1 and GluN2B was significantly higher in each drug-treated group ($p<0.05$), with high-dose group experiencing the most significant increase ($p<0.05$). In comparison to the MEM group, high-dose and medium-dose groups showed greater expression of GluA2, GluN1 and GluN2B ($p<0.05$). High-dose group considerably outperformed the MEM group in terms of GluA2, GluN1 and GluN2B expression ($p<0.05$). However, the difference between the medium-dose group

and MEM group were not statistically significant (p>0.05) (Table 5).

Effect on synapse-associated proteins was compared. Compared with the sham group, the expression levels of GAP-43, Syn and PSD-95 in the hippocampus of the model group were significantly lower (p<0.05). Compared with the model group, the expression levels of all dosing groups were significantly higher (p<0.05), with the most significant increase in the high-dose group of TQYZG, and the protein expression levels of the high-dose group were not significantly different from those of the sham group (p>0.05). The difference between the TQYZG medium-dose group and MEM group was not statistically significant (p>0.05) (fig. 4 and Table 6).

Effect of TQYZG on Mitogen Activated Protein Kinase/Extracellular signal Regulated Kinase 1/2 (MAPK/ERK) pathway in VaD rats was evaluated. The expression levels of MEK1/2, ERK1/2 and CERB in each group were not statistically significant (p>0.05). Compared with the sham group, the expression levels of p-MEK1/2, p-ERK1/2 and p-CERB in the hippocampus of the model group were reduced (p<0.001). Similarly, compared with the model group the expression levels of p-MEK1/2, p-ERK1/2 and p-CREB in each administration group increased (p<0.05). However, the expression levels of p-MEK1/2, p-ERK1/2 and p-CREB in each administration group were not statistically significant compared with the model group (p<0.05). Additionally, p-CREB levels increased in all dosing groups (p<0.05), with most significant increase in the high-dose group (p<0.05). The difference in protein expression levels between the MEM and medium-dose groups were not statistically significant (p>0.05) (fig. 5 and Table 7).

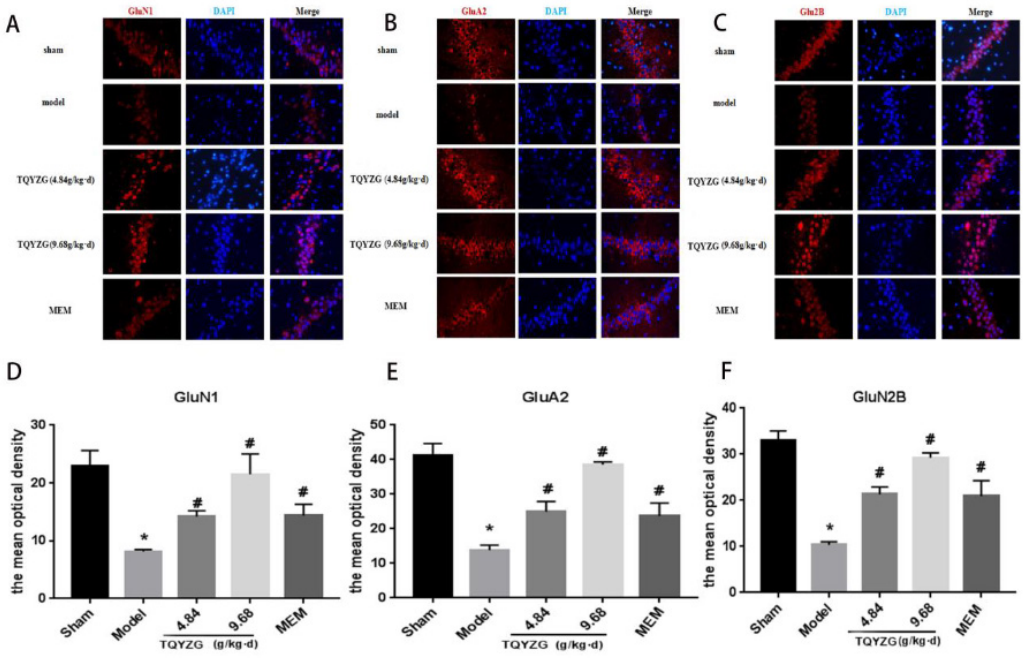


**Fig. 3: (A): Fluorescent staining and (B): Expression of GluA2, GluN1 and GluN2B in the hippocampus of various groups of rats**

**TABLE 5: RESULTS OF FLUORESCENCE EXPRESSION OF GLUA2, GLUN1 AND GLU2B IN THE HIPPOCAMPUS OF RATS IN EACH GROUP (n=5, x̄±s)**

| Group | GluA2 (MOD) | GluN1 (MOD) | GluN2B (MOD) |
|---|---|---|---|
| Sham | 41.33±3.328 | 22.936±2.69 | 32.966±2.096 |
| Model | 13.793±1.466*+♦□ | 8.144±0.344*+♦□ | 10.38±0.624*+♦□ |
| TQYZG medium-dose | 24.93±2.949*#+ | 14.177±1.007*#+ | 29.253±1.609*#+ |
| TQYZG high-dose | 38.577±0.751*#♦□ | 21.49±3.538*#♦□ | 29.253±1.066*#♦□ |
| MEM | 23.733±10.776*#+ | 14.366±1.962*#+ | 22.962±2.576*#+ |
| F | 53.777 | 22.05 | 57.447 |
| p | <0.01 | <0.01 | <0.01 |

Note: *p<0.05 *vs*. sham group, #p<0.05 *vs*. model group, +p<0.05 *vs*.TQYZG high dose group, ♦p<0.05 *vs*. TQYZG medium-dose group and □p<0.05 *vs*. MEM group

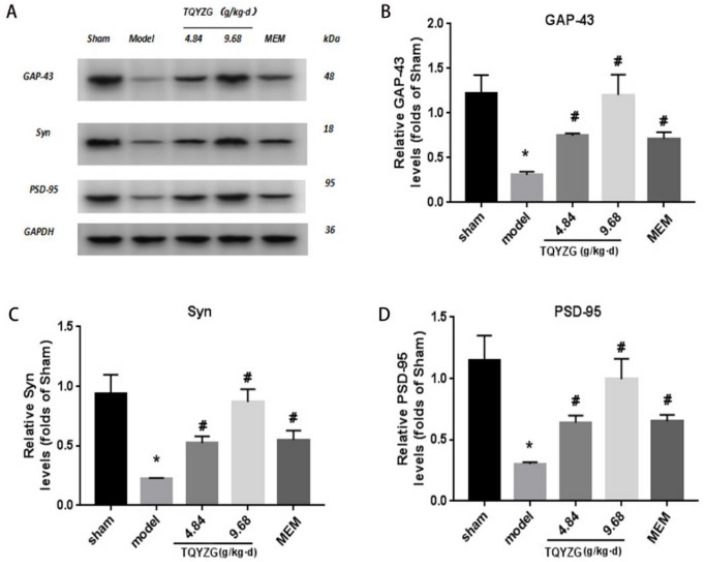


**Fig. 4: Immunofluorescence and expression levels in hippocampal tissues of various groups of rats, (A): TQYZG; (B): GAP-43; (C): Syn and (D): PSD-95**

**TABLE 6: EXPRESSION LEVELS OF SYNAPTIC-RELATED PROTEINS IN THE HIPPOCAMPUS OF EACH GROUP OF RATS (n=5, x̄±s)**

| Group | GAP-43 | Syn | PSD-95 |
|---|---|---|---|
| Sham | 1.22±0.203 | 0.94±0.155 | 1.15±0.20 |
| Model | 0.31±0.0345*♦□ | 0.27±0.322*♦□ | 0.30±0.15*+♦□ |
| TQYZG medium-dose | 0.74±0.0271*# | 0.59±0.106*# | 0.64±0.57*#+ |
| TQYZG high-dose | 1.20±0.226*#♦□ | 0.87±0.11*#♦□ | 0.99±0.17*#♦□ |
| MEM | 0.711±0.073*# | 0.45±0.74*# | 0.65±0.45*#+ |
| F | 22.081 | 20.226 | 22.298 |
| p | <0.01 | <0.01 | <0.01 |

Note: *p<0.05 *vs*. sham group, #p<0.05 *vs*. model group, +p<0.05 *vs*.TQYZG high dose group, ♦p<0.05 *vs*. TQYZG medium-dose group and □p<0.05 *vs*. MEM group

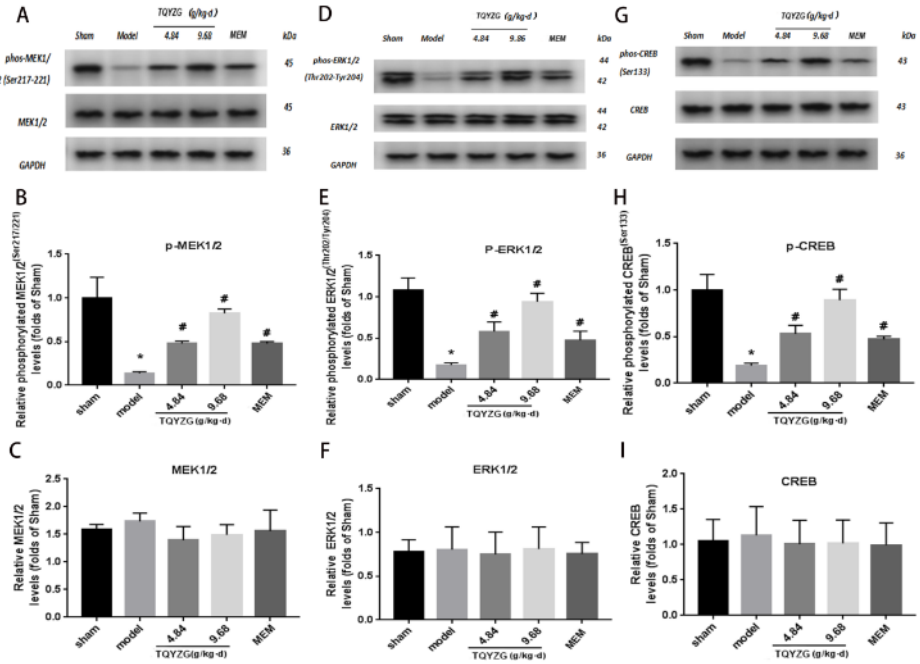


**Fig. 5: Immunofluorescence and expression levels of key proteins of the MAPK/ERK pathway in the hippocampus of various groups of rats, (A): Immunofluorescence of MEK; (B): p-MEK1/2; (C): MEK1/2; (D): Immunofluorescence of ERK; (E): p-ERK1/2; (F): ERK1/2; (G): immunofluorescence of CREB protein; (H): p-CREB and (I): CREB**

**TABLE 7: EXPRESSION LEVELS OF KEY PROTEINS OF MAPK/ERK PATHWAY IN THE HIPPOCAMPUS OF EACH GROUP OF RATS (n=5, x̄±s)**

| Group | p-MEK1/2 | MEK1/2 | p-ERK1/2 | ERK1/2 | p-CREB | CREB |
|---|---|---|---|---|---|---|
| Sham | 1.0±0.24 | 1.0±0.06 | 1.07±0.15 | 1±0.17 | 1±0.17 | 1±0.29 |
| Model | 0.14±0.02*+♦□ | 1.09±0.1 | 0.18±0.24*+♦□ | 1.03±0.33 | 0.19±0.03*+♦□ | 1.08±0.38 |
| TQYZG medium-dose | 0.47±0.03*#♦ | 0.88±0.15 | 0.58±0.12*#♦ | 0.96±0.32 | 0.53±0.09*#♦ | 0.96±0.32 |
| TQYZG high-dose | 0.82±0.05*#+□ | 0.94±0.12 | 0.94±0.10*#+□ | 1.04±0.32 | 0.89±0.12*#+□ | 0.97±0.31 |
| MEM | 0.48±0.02*#♦ | 0.98±0.24 | 0.47±0.11*#♦ | 0.94±0.16 | 0.47±0.03*#♦ | 0.95±0.30 |
| F | 18.1 | 0.8594 | 19.26 | 0.05107 | 31.45 | 0.08287 |
| p | <0.001 | 0.5202 | <0.001 | 0.9943 | <0.001 | 0.9858 |

Note: *p<0.05 *vs*. sham group, #p<0.05 *vs*. model group, +p<0.05 *vs*.TQYZG high dose group, ♦p<0.05 *vs*. TQYZG medium-dose group and □p<0.05 *vs*. MEM group

Chronic underperfusion of brain tissue is the primary cause of VaD, an illness which is defined by cognitive impairment brought on by cerebrovascular disorders such cerebral ischemia and cerebral hemorrhage. Two-Vessel Occlusion (2-VO) technique, a dependable animal model for chronic hypoperfusion-induced vascular dementia, was used to create the animal model for the experiment[9]. At the same time, 2-VO animal model causes chronic hypoperfusion in the entire brain after surgery, which can result in neuroinflammatory responses, deletion and damage to hippocampal neurons as well as synaptic and dendritic lesions[10,11], which are strikingly similar to the pathological state and symptoms in the brains of VaD patients. A considerable rise in EL values in the modeled rats compared to the sham operation, exhibiting longer escape duration, indicates effective modeling in this experiment's behavioral assessment of the rats utilizing the MWM for 1 mo, following surgery.

Numerous investigations have demonstrated a strong correlation between VaD development and impaired synaptic plasticity[12]. After cerebral ischemia, synaptic disruption and damage are regarded to be the primary causes of cognitive impairments. High degree of plasticity and flexibility that synaptic structures exhibit influences the effectiveness of synaptic transmission and synaptic tructures, which in turn impacts memory capacity. The transmission of signals or abnormal behavior is influenced by the plasticity of synaptic ultrastructure[13]. In this study, we showed that TQYZG can enhance the plasticity of synaptic ultrastructure by safeguarding the integrity of synaptic ultrastructure, which can effectively prevent synaptic loss and protect synaptic transmission efficacy by remodeling a synaptic structure, thereby enhancing the morphology and density of dendritic spines. As a result, VaD rats' learning and memory abilities can be improved.

One of the processes through which memory impairment manifests in VaD is suppression of the MAPK/ERK signaling pathway following chronic cerebral hypoperfusion, accompanied by decreased activity of the pathway cascade components namely, MEK, ERK and CREB. The biological foundation of long-term memory is Long Time Potentiation (LTP), which is intimately related to synaptic plasticity and learning memory[14]. Synaptic plasticity, learning and memory are initiated and regulated by the MAPK/ERK signaling pathway and the expression of LTP influences the expression of GluA2 as well. Neuronal differentiation and survival are regulated by CREB phosphorylation and its aftereffects. In synaptic cells, CREB is a crucial transcription factor, and ERK is one of its upstream regulators. A substantial amount of data points to the crucial role that CERB's phosphorylation plays an important role in learning and memory; phosphorylation site anti-phospho-CREB (Ser133) directly controls the transcription of early genes involved in learning and memory, including fos-proto-oncogene-(c-fos) and jun-proto-oncogene (c-jun)[15].

Our research revealed that the hippocampus of the model group rats displayed significantly lower levels of p-MEK1/2, p-ERK1/2 and p-CERB expression. TQYZG intervention improved the decreasing trend of p-MEK1/2, p-ERK1/2 and p-CERB, and the reversal was at high doses. Total MEK1/2, ERK1/2 and CERB proteins remained basically unaltered in the whole hippocampus both before and after treatment. While high and medium dosages of TQYZG restored the decrease of p-MEK1/2 and p-ERK1/2. Lower phosphorylation levels of ERK and MEK imply that reduced phosphorylation of MEK1/2 and ERK1/2 in the hippocampus is sufficient to produce memory impairment, leading to VaD. The phosphorylated form of CREB is a key factor in memory impairment following chronic

cerebral hypoperfusion and treatment with TQYZG prevented the decrease of p-CREB and relieved VaD symptoms. Meanwhile, CERB, a downstream gene of the MAPK/ERK pathway, decreased the phosphorylation levels in VaD rats but total protein CREB did not. High-dose group of TQYZG was the best for all of the aforementioned therapies.

NMDA, AMPA, and other GluA2 are a class of ligand-gated ion channels that mediate rapid excitatory transmission and are important players in synaptic LTP. Synaptic plasticity is widely recognized as the physiological basis of learning and memory, glutamate-mediated excitatory transmission is disrupted, and synaptic loss is particularly severe for glutamatergic neurons[16]. The N-Methyl-D-Aspartic acid Receptor (NMDAR), the AMPAR (Amino-3-hydroxy-5-Methyl-4-isoxazole Propionic Acid Receptor), and red alginate are three subfamilies that belong to them[17]. The central nervous system has many competent glutamate receptors, such as NMDA and AMPA receptors, which promote synaptic plasticity and regulate information stored in the brain.

In the present experiment, we focused on the NMDAR subunits GluN1 and Glu2B and the AMPAR subunit GluA2 and the results showed that the expression of GluN1, Glu2B, and GluA2 in the CA1 region was downregulated in the hippocampal tissues of demented rats after fluorescence quantitative staining analysis, while there was a different degree of increase in the intervention and medium and high dose groups. The protective memory function of TQYZG was found to be accomplished by encouraging the expression of excitatory amino acid receptors in the post-synaptic membrane of the hippocampus of VaD model rats, thereby increasing the synaptic transmission efficacy, in conjunction with the findings of synaptic ultrastructural morphology and neuronal dendritic spine density.

In addition, it has been proposed that one of the mechanisms causing dementia is the presence of significant protein factors on synaptic membranes, such as PSD-95 and Syn, whose expression is downregulated following decreased cerebral perfusion[18]. A key synapse component located in the postsynaptic terminal's active region, PSD-95 is a marker of synaptic structure whose expression level can roughly correspond to the number of synapses. PSD-95, is a crucial protein in regulating signal transduction while LTP is involved in learning and memory; it is inactive on its own, binds to glutamate receptors and indirectly controls AMPA receptor trafficking and expression[19]. Syn is a crucial marker of synapses and plays a significant role in the transit, docking, and release of synaptic vesicles and their contents. GAP-43, like Syn, is a presynaptic protein with a wide distribution, especially in axon growth cones, plays a key role in the cytoskeleton dynamics of axon growth, guidance and synapse formation; it is also a molecular marker of neuronal axon regeneration.

When TQYZG were administered, the expression of PSD-95, Syn and GAP-43 significantly increased suggesting that it can promote synaptic remodeling and neural regeneration by up-regulating the expression of PSD-95, Syn and GAP-43, protecting memory and learning.

Based on the results of the experiments, we postulate that TQYZG can enhance the ultrastructure of hippocampal synapses in VaD rats, increase the density of neuronal dendritic spines and thereby enhance the plasticity of synaptic structures. Moreover it can also enhance the content of excitatory glutamate receptor subunits GluN1, GluN2B and GluA2 on synaptic membranes, to increase synaptic plasticity and improve synaptic transmission, and upregulate the expression of GAP-43, Syn and PSD-95. In addition to improving synaptic plasticity and transmission efficiency, PSD-95 expression improves learning and memory by influencing the hippocampus's MAPK/ERK signaling cascade, activating important components and encouraging downstream CREB activation.

**Conflict of interests:**

The authors declared no conflict of interests.

## REFERENCES


1. Sinha K, Sun C, Kamari R, Bettermann K. Current status and future prospects of pathophysiology-based neuroprotective drugs for the treatment of vascular dementia. Drug Discov Today 2020;25(4):793-99.
2. Thal DR, Grinberg LT, Attems J. Vascular dementia: Different forms of vessel disorders contribute to the development of dementia in the elderly brain. Exp Gerontol 2012;47(11):816-24.
3. Lee LL, Aung HH, Wilson DW, Anderson SE, Rutledge JC, Rutkowsky JM. Triglyceride-rich lipoprotein lipolysis products increase blood-brain barrier transfer coefficient and induce astrocyte lipid droplets and cell stress. Am J Physiol Cell Physiol 2017;312(4):500-16.
4. Zhu NW, Yin XL, Lin R, Fan XL, Chen SJ, Zhu YM, *et al*. Possible mechanisms of lycopene amelioration of learning and memory impairment in rats with vascular dementia. Neural Regen Res 2020;15(2):332-41.
5. van Charante EP, Richard E, Eurelings LS, van Dalen JW,

Ligthart SA, van Bussel EF, *et al*. Effectiveness of a 6 y multidomain vascular care intervention to prevent dementia (preDIVA): A cluster-randomised controlled trial. Lancet 2016;388(10046):797-805.
6. Javanshiri K, Waldo ML, Friberg N, Sjovall F, Wickerstrom K, Haglund M, *et al*. Atherosclerosis, hypertension, and diabetes in Alzheimer's disease, vascular dementia, and mixed dementia: Prevalence and presentation. J Alzheimers Dis 2018;65(4):1247-58.
7. Appleton JP, Scutt P, Sprigg N, Bath PM. Hypercholesterolaemia and vascular dementia. Clin Sci 2017;131(14):1561-78.
8. Ohta H, Nishikawa H, Kimura H, Anayama H, Miyamoto M. Chronic cerebral hypoperfusion by permanent internal carotid ligation produces learning impairment without brain damage in rats. Neuroscience 1997;79(4):1039-50.
9. Jiwa NS, Garrard P, Hainsworth AH. Experimental models of vascular dementia and vascular cognitive impairment: A systematic review. J Neurochem 2010;115(4):814-28.
10. Vicente É, Degerone D, Bohn L, Scornavaca F, Pimentel A, Leite MC, *et al*. Astroglial and cognitive effects of chronic cerebral hypoperfusion in the rat. Brain Res 2009;1251:204-12.
11. Buckley EM, Patel SD, Miller BF, Franceschini MA, Vannucci SJ. *In vivo* monitoring of cerebral hemodynamics in the immature rat: Effects of hypoxia-ischemia and hypothermia. Dev Neurosci 2015;37(4-5):407-16.
12. Liu B, Liu J, Zhang J, Mao W, Li S. Effects of autophagy on synaptic-plasticity-related protein expression in the hippocampus CA1 of a rat model of vascular dementia. Neurosci Lett 2019;707:1-5.
13. Eltokhi A, Santuy A, Merchan-Perez A, Sprengel R. Glutamatergic dysfunction and synaptic ultrastructural alterations in schizophrenia and autism spectrum disorder: Evidence from human and rodent studies. Int J Mol Sci 2020;22(1):1-17.
14. Rajendran L, Paolicelli RC. Microglia-mediated synapse loss in Alzheimer's disease. J Neurosci 2018;38(12):2911-19.
15. Tischmeyer W, Kaczmarek L, Strauss M, Jork R, Matthies H. Accumulation of c-fos mRNA in rat hippocampus during acquisition of a brightness discrimination. Behav Neural Biol 1990;54(2):165-71.
16. Gong T, Luo Z, Huang L, Xiao C, Yi J, Yan J, *et al*. Effect and mechanism of Yisui Fuyongtang (YSFYT) decoction on cognitive function and synaptic plasticity in rats with vascular cognitive impairment. J Immunol Res 2022:1-17.
17. Francis PT. Glutamatergic systems in Alzheimer's disease. Int J Geriatr Psychiatry 2003;18:15-21.
18. Traynelis SF, Wollmuth LP, McBain CJ, Menniti FS, Vance KM, Ogden KK, *et al*. Glutamate receptor ion channels: Structure, regulation, and function. Pharmacol Rev 2010;62(3):405-96.
19. Kutsuwada T, Kashiwabuchi N, Mori H, Sakimura K, Kushiya E, Araki K, *et al*. Molecular diversity of the NMDA receptor channel. Nature 1992;358(6381):36-41.



**This article was originally published in a special issue, "Drug Discovery and Repositioning Studies in Biopharmaceutical Sciences" Indian J Pharm Sci 2024:86(4) Spl Issue "241-251"**